18th International Conference on Information Fusion
Washington, DC - July 6-9, 2015

# Dynamic-Occlusion Likelihood Incorporation in a PHD Filter Based Range-Only Tracking System

Snezhana Jovanoska* †, Felix Govaers*, Reiner Thomä†, Wolfgang Koch*
* Department of Sensor Data and Information Fusion (SDF), Fraunhofer FKIE,
Fraunhoferstrasse 20, 53343 Wachtberg, Germany
† Electronic Measurements Research Lab, Institute of Information Technology, Ilmenau university of Technology,
Helmholtz Ring 2, 98684 Ilmenau, Germany
Correspondence: snezhana.jovanoska@tu-ilmenau.de

***Abstract*—In multiple target tracking target occlusion or shadowing is a common occurrence. A target may be occluded by an existing structure, or in many cases, by another moving target in the environment. In this paper we consider a UWB-based range-only person tracking system. Occlusion regions induced by moving targets in the scenario are defined followed by a derivation of an occlusion likelihood function. The occlusion likelihood is then incorporated within a person localization and tracking framework based on the PHD filter by influencing the probability of target detection. Numerical and experimental results demonstrate that the incorporation of 'negative information' leads to a more complete belief of the scenario and can result in use of fewer sensors for covering the area of interest.**

## I. Introduction

In most localization and tracking techniques only positive information, i.e. target features observed by the sensors, is used. However, additional information is available from scenario areas that should be observed by the sensor but no measurements are available due to possible occlusions of the targets present in these areas. Negative information describes the general case that no targets were detected in the field of view of the sensor. According to [1] measurements can be missing if an expected object is out of range, occluded or due to sensor failure. It is suggested that false interpretation of negative information can be avoided by modeling the measurement process as exactly as possible and considering occlusions by dynamic or static objects in the scenario.

Negative information is commonly used in robotics [2] in occupancy grid mapping. In [3], a centralized occupancy grid is generated from multiple cooperative sensors and used to confirm the tracking results by discarding tracks in unoccupied regions. [4] uses negative information to address sensor limitations such as Doppler blindness, jamming, finite resolution etc. In localization, negative information is used in [1] for particle filter based localization in a known map and in [5] for tracking known number of objects in a known map. Analytic model of occlusion is presented in [6], where a penalty cost is defined for unresolved tracks dependent on the modeled track visibility. In [7] an occlusion likelihood model is derived for occlusions created by dynamic extended targets. Utilization of the occlusion information improves the accuracy and sensibility of state estimates for occluded objects.

In this paper we consider localization and tracking of multiple tag-free persons as in our work in [8], [9], where persons are detected by the changes they impose in the channel impulse response (CIR) measured with a transmitter-receiver pair of a ultra-wideband (UWB) module. The time of arrival (ToA) (or correspondingly return range) of the persons can be estimated and used for localization. When referring to range here we actually refer to the return range i.e. the distance traveled by the signal from the transmitter to the target and back to the receiver. In the presence of multiple persons, a person close to the transmitter or receiver of the sensor 'shadows' the persons located behind it with respect to the sensor since UWB signals are strongly attenuated after scattering from a person. Occlusions results in missing or incomplete measurements and are a serious challenge for extended multi-target tracking. Shadowing influences on UWB sensors are studied in [10]. In [8], [9], multiple UWB sensors distributed around the area of interest are used to counteract the shadowing influences. It is assumed that persons that can not be observed by one sensor would be observed by another sensor of the network.

In [11] a geometry based occlusion model was introduced and a simple occlusion handling procedure was applied. The results show that an occlusion handling procedure highly benefits the overall person localization and tracking procedure. In this paper we extend the models presented in [11], derive an occlusion likelihood function (Section III) and incorporate it within a PHD filter based person tracking system in Section IV. The proposed method is numerically and experimentally verified in Section V.

## II. Occlusion Modeling

The occlusion region of a detected person is a region in the scenario where other persons/targets can not be detected due to the strong attenuation of the UWB signals caused by this person. For a known person location and extent and known sensor positions, the occlusion region can be modeled as the area behind the detected target with respect to the sensor.

Since only the range information of the target is used as observed by the UWB sensor, the location, extent and direction of that target need to be estimated and/or approximated from the target tracking procedure. A person in 2D can be approximated as an elliptical target if the direction of movement is known.

For simplicity, we here approximate the target as a circle with diagonal equal to the major axis of a target extent ellipse.

Lets assume that a target $m$ can be modeled by a circle with radius $r^m$ and center $(x^m, y^m)$ (blue dashed circle in Fig. 1). Let the observed target range be $d^m$ (represented by the black ellipse in Fig. 1). The target range is represented by an ellipse due to the bistatic configuration of the transmitting and receiving antennas. The target extent limits with respect to the sensor can be determined as the intersection points of the circle representing the target and the range ellipse (the two black points in Fig. 1). These intersection points can be determined by solving the two equations:

$$r^m = \sqrt{(x^m - x)^2 + (y^m - y)^2} \tag{1}$$

$$\begin{aligned} d^m = &\sqrt{(x - x^{Tx})^2 + (y - y^{Tx})^2} \\ &+ \sqrt{(x - x^{Rx})^2 + (y - y^{Rx})^2} \end{aligned} \tag{2}$$

where $(x^{Tx}, y^{Tx})$ and $(x^{Rx}, y^{Rx})$ are the coordinates of the transmitter and receiver respectively.

To determine the region shadowed by target $m$ we need to determine the left and right cut-off lines. They are determined by the line passing through one of the antennas and one of the points we determined above (light gray dotted lines in Fig. 1). The modeled occlusion region is limited to the field of view of the sensor.

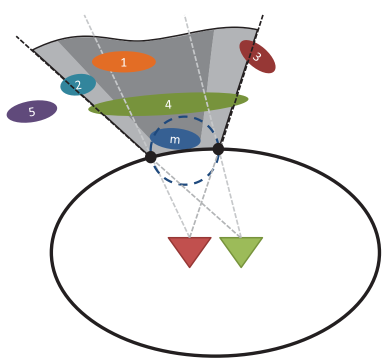


Fig. 1. Occlusion region of a target: the modeled occlusion region (light gray) and the true occlusion region (dark gray) - target 1 (orange) is fully shadowed, targets 2, 3, and 4 are partially shadowed by target m (dark blue), and target 5 (purple) may be observed by the sensor

The true size, shape and orientation of the object influence the accuracy of this model. Any inaccuracies result in a conservative likelihood, guaranteeing that the true shadow is a subset of this approximation and is not mistaken to be visible.

In a generalized case, an arbitrary number of tracked targets exist, and each of them generates a shadow over the field of view. To avoid duplicates, the likelihood that target $n$ is shadowed is defined as the likelihood that target $n$ is shadowed by the target with minimum range to the sensor that also shadows target $n$.

## III. Occlusion Likelihood

To determine the occlusion likelihood at a given point in time, the estimated location and extent of the present targets is needed. In the above section the occlusion region is modeled geometrically. Here we give the minimum conditions that need to be satisfied to define the occlusion region analytically. This is similar to the modeled likelihood in [7], with the difference that in [7] range and bearing measurements are available, and here we only have range measurements and model the target extent to obtain the angular extent of a target.

Object $n$ is shadowed by object $m$ if $m$ is closer to the sensor compared to $n$, i.e. $R^{n,m} = (d^n \geq d^m)$, and the angular extend of object $n$ is smaller than the extent of object $m$ with respect to the sensor position, i.e. $B_1^{n,m} = (\theta^n \geq \theta^m) \cap (\phi^m \geq \phi^n)$, where $\theta^i$ is the clockwise angular extent of object $i$ and $\phi^i$ is the counter clockwise angular extent of object $i$. The angular extent of the objects is always calculated positive clockwise from the x-axis. The probability that object $n$ is fully occluded by object $m$, $O^{n,m}$, assuming $R^{n,m}$ and $B_1^{n,m}$ are independent of each other, is then defined as:

$$p(O^{n,m}) = p(E^m)\, p(R^{n,m}|E^m)\, p(B_1^{n,m}|E^m) \tag{3}$$

where $p(E^m)$ is the probability that object $m$ exists. The range

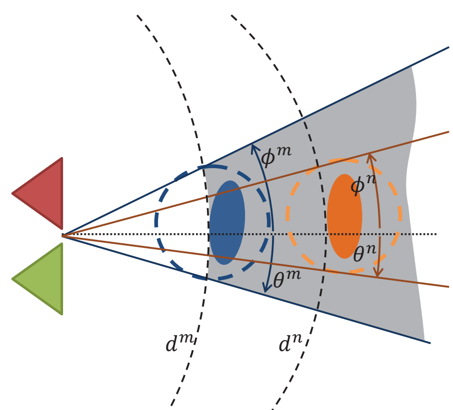


Fig. 2. Full occlusion diagram of a target and defining parameters

and angular extent probabilities are computed using a smooth transition function based on the hyperbolic tangent function, i.e.

$$\begin{aligned} p(R^{n,m}|E^m) &= s\left(\frac{d^n - d^m}{\sqrt{\sigma_{d^n}^2 + \sigma_{d^m}^2}}\right) \\ p(B_1^{n,m}|E^m) &= s\left(\frac{\theta^n - \theta^m}{\sqrt{\sigma_{\theta^n}^2 + \sigma_{\theta^m}^2}}\right)\, s\left(\frac{\phi^m - \phi^n}{\sqrt{\sigma_{\phi^n}^2 + \sigma_{\phi^m}^2}}\right) \end{aligned} \tag{4}$$

where

$$s(x) = \frac{1}{2} + \frac{1}{2}\tanh(x) \tag{5}$$

Analogous to the occlusion model in [7], we extend the occlusion likelihood function to also cover the cases of partially occluded targets such as targets 2, 3, and 4 in Fig. 1. For these cases additional angular extent conditions are defined i.e.

$$\begin{aligned} B_2^{n,m} &= (\phi^m \geq \theta^n) \cap (\phi^n \geq \phi^m) \\ B_3^{n,m} &= (\theta^m \geq \theta^n) \cap (\phi^n \geq \theta^m) \end{aligned} \tag{6}$$

where $B_2^{n,m}$ is the condition for partially occluded targets on the left of the occlusion region (covering case 2 and 4 from Fig 1) and $B_3^{n,m}$ is the condition for partially occluded targets on the right of the occlusion region (covering case 3 and 4 from Fig 1).

Since $B_2^{n,m}$ and $B_3^{n,m}$ both include case 4, they are not mutually exclusive. Thus the partial occlusion likelihood is

$$p(O^{n,m}) = p(E^m)\, p(R^{n,m}|E^m)\, p(B^{n,m}|E^m) \tag{7}$$

where

$$\begin{aligned} p(B^{n,m}|E^m) &= p(B_1^{n,m} \cup B_2^{n,m} \cup B_3^{n,m}|E^m) \\ &= p(B_1^{n,m}|E^m) + p(B_2^{n,m}|E^m) + ... \\ &\quad p(B_3^{n,m}|E^m) - p(B_2^{n,m} \cap B_3^{n,m}|E^m) \end{aligned} \tag{8}$$

and

$$\begin{aligned} p(B_2^{n,m}|E^m) &= s\left(\frac{\phi^m - \theta^n}{\sqrt{\sigma^2_{\phi^m} + \sigma^2_{\theta^n}}}\right) s\left(\frac{\phi^n - \phi^m}{\sqrt{\sigma^2_{\phi^n} + \sigma^2_{\phi^m}}}\right) \\ p(B_3^{n,m}|E^m) &= s\left(\frac{\theta^m - \theta^n}{\sqrt{\sigma^2_{\theta^m} + \sigma^2_{\theta^n}}}\right) s\left(\frac{\phi^n - \theta^m}{\sqrt{\sigma^2_{\phi^n} + \sigma^2_{\theta^m}}}\right) \\ p(B_2^{n,m} \cap B_3^{n,m}|E^m) &= ... \\ & s\left(\frac{\theta^m - \theta^n}{\sqrt{\sigma^2_{\theta^m} + \sigma^2_{\theta^n}}}\right) s\left(\frac{\phi^n - \phi^m}{\sqrt{\sigma^2_{\phi^n} + \sigma^2_{\phi^m}}}\right) \end{aligned} \tag{9}$$

In the general case of arbitrary number of tracked targets, $N$, the total occlusion likelihood of object $n$ is

$$p(O^n) = \bigcup_{m=1, m \neq n}^{N} p(O^{n,m}) \tag{10}$$

Since an object $n$ may be occluded by multiple targets simultaneously, the events in (10) are not mutually exclusive. Thus (10) is expanded as in [7]:

$$p(O^n) = \sum_{i=1}^{N-1} \left\{ (-1)^{(i+1)} \sum_{j=1}^{^{(N-1)}C_i} \left[ \prod_{k=1}^{i} p\left(O^{n,\mathbb{C}_j^i(k)}\right) \right] \right\} \tag{11}$$

where $\mathbb{C}_j^i(k)$ is the $k$-th object in the $j$-th $i$-combination and $^{(N-1)}C_i$ is the number of $i$-combinations in the set of $N-1$ tracked targets (all targets excluding $n$).

The complement of the occlusion likelihood is the detection likelihood, i.e. the likelihood that target $n$ is fully visible to the sensor

$$p(\overline{O^n}) = 1 - p(O^n) \tag{12}$$

## IV. Occlusion Information Fusion

The occlusion model and likelihood function presented above are integrated within the PHD filter as shown in Fig. 3. The 'Feature extraction' block estimates the ranges from the raw measurements which are then used as observations in the tracker. The range estimation procedure is explained in [9]. An observation dependent birth model for the target birth intensity is used as in [11]. Since each transmitter-receiver pair is considered as separate sensor, a multi-sensor update equations are used in the PHD filter. This is the way the conventional PHD filter is defined. In the modified PHD filter we use the 'Occlusion likelihood definition' block to define the probability of target occlusion based on the predicted target states, and integrate it within the 'Measurement update' block.

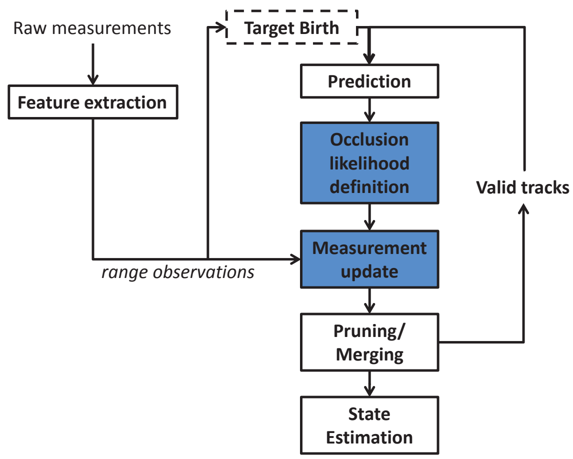


Fig. 3. Block diagram of the modified multi-target tracker

### A. The Conventional PHD Filter

The target tracking problem can be summarized as an estimation of the number of targets and their states (locations) at each point in time using a set of noisy measurements and the information of the previous target states. In finite set statistics terminology, at a given time $t$, the random finite set (RFS) of targets states is $X_t = \{\mathbf{x}_t^{(i)}\}_{i=1}^{N_{x,t}}$ and the RFS of measurements is $Z_t = \{\mathbf{z}_t^{(i)}\}_{i=1}^{N_{z,t}}$, where $N_{x,t}$ is the estimated number of targets at time $t$ and $N_{z,t}$ is the number of available measurements at time $t$. Each $\mathbf{z}_t^{(i)}$ is either a noisy observation of one of the targets or clutter. Each target state is represented by $\mathbf{x}_t^{(i)}$. The set-based approach allows for varying number of targets to appear and disappear without any particular order while avoiding explicit data association.

The probability hypothesis density is the first moment of the multi-target posterior distribution. It is a multi-modal distribution over the target space and each mode, or peak, represents a high probability of target presence. Since at a given time the target states are considered to be a set-valued state, it operates on single target state space and avoids the complexities arising from data association. It is not a probability density function and does not integrate to unity. Its integration over a finite subset of the space gives an estimated number of the targets in this subset. The propagation of the posterior intensity function $v_t$ uses the following recursion:

$$v_{t|t-1}(\mathbf{x}_t) = \int \phi_{t|t-1}(\mathbf{x}_t, \zeta)\, v_{t-1}(\zeta)\, d\zeta + \gamma_t(\mathbf{x}_t) \tag{13}$$

$$\begin{aligned} v_t(\mathbf{x}_t) &= [1 - p_{D,t}(\mathbf{x}_t)] v_{t|t-1}(\mathbf{x}_t) \\ &+ \sum_{\mathbf{z}_t \in Z_t} \frac{\psi_{t,z}(\mathbf{x}_t)\, v_{t|t-1}(\mathbf{x}_t)}{\kappa_t(\mathbf{z}_t) + \int \psi_{t,z}(\zeta)\, v_{t|t-1}(\zeta)\, d\zeta} \end{aligned} \tag{14}$$

The transition density in (13) is defined as:

$$\phi_{t|t-1}(\mathbf{x}_t, \zeta) = p_{S,t}(\zeta)\, f_{t|t-1}(\mathbf{x}_t|\zeta) + \beta_{t|t-1}(\mathbf{x}_t|\zeta) \tag{15}$$

where $f_{t|t-1}(\mathbf{x}_t|\mathbf{x}_{t-1})$ is the single target transition density, $p_{S,t}(\mathbf{x}_{t-1})$ is the probability of survival, $\beta_{t|t-1}(\mathbf{x}_t|\mathbf{x}_{t-1})$ is the PHD for spawned target birth and $\gamma_t(\mathbf{x}_t)$ is the PHD for spontaneous birth of new targets at time $t$. In the update equation (14), $\psi_{t,z}(\mathbf{x}_t) = p_{D,t}(\mathbf{x}_t)\, g(\mathbf{z}_t|\mathbf{x}_t)$, where $g$ is the single target likelihood function and $p_{D,t}(\mathbf{x}_t)$ is the probability of detection. The intensity of clutter points is defined as $\kappa_t(\mathbf{z}_t) = \lambda_t c_t(\mathbf{z}_t)$, where $\lambda_t$ is the Poisson parameter defining the expected number of false alarms and $c_t(\mathbf{z}_t)$ is the probability distribution over the measurement space.

The main assumptions of the PHD filter are independence of the measurements generated by each target, independence of clutter from target-based measurements, and that the predicted RFS is Poisson.

Generalizations of the single-sensor PHD filter to a multiple sensor case have been originally proposed by Mahler in [12]. The update equation is however too complicated to be of practical use. Different multiple sensor approximations are presented in [13]. The most common approach is to apply the single sensor update equation multiple times in succession as in [14]. The update equation of the multiple sensor PHD filter is then approximated as:

$$v_t(\mathbf{x}_t) = v_{t|t-1}^{[N]}(\mathbf{x}_t) \tag{16}$$

where $N$ is the number of sensors used. For the $j$-th sensor we have:

$$\begin{aligned} v_{t|t-1}^{[j]}(\mathbf{x}_t) &= [1 - p_{D,t}^{[j]}(\mathbf{x}_t)] v_{t|t-1}^{[j-1]}(\mathbf{x}_t) \\ &+ \sum_{\mathbf{z}_t \in Z_t^{[j]}} \frac{\psi_{t,z}^{[j]}(\mathbf{x}_t)\, v_{t|t-1}^{[j]}(\mathbf{x}_t)}{\kappa_t^{[j]}(\mathbf{z}_t) + \int \psi_{t,z}^{[j]}(\zeta)\, v_{t|t-1}^{[j]}(\zeta)\, d\zeta} \end{aligned} \tag{17}$$

where

$$\begin{aligned} v_{t|t-1}^{[0]}(\mathbf{x}_t) &= v_{t|t-1}(\mathbf{x}_t) \\ \psi_{t,z}^{[j]}(\mathbf{x}_t) &= p_{D,t}^{[j]}(\mathbf{x}_t)\, g^{[j]}(\mathbf{z}_t|\mathbf{x}_t) \end{aligned} \tag{18}$$

$p_{D,t}^{[j]}(\mathbf{x}_t)$ is the probability of detection of sensor $j$, $Z_t^{[j]}$ is the set of acquired measurements by sensor $j$ at time $t$, $\kappa_t^{[j]}(z)$ is the clutter intensity for sensor $j$ and $g^{[j]}$ is the single target likelihood function of sensor $j$.

The sequential PHD filter is highly dependent on the order the sensors are used. Thus if sensor 'reliability' is known or computed, the observations of the most 'reliable' sensors should be used first.

To avoid the sensor order dependency, the sequential PHD filter can be applied over all possible sensor orders. This can be very expensive when many sensors are used. The updated intensities of the different sensor orders can then be merged. We have to note that before merging the intensity obtained from the different sensor orders a normalization with the number of possible sensor order permutations should be applied.

In this work we use the Gaussian Mixture implementation of the PHD filter (GMPHD) [15]. Target spawning is omitted for simplicity. The number of Gaussian mixtures (GMs) in $v_t(\mathbf{x}_t)$ is $J_t = (J_{t-1} + J_{\gamma,t})\left(1 + |Z_t^{[1]}|\right) \ldots \left(1 + |Z_t^{[N]}|\right)$ has an almost exponential growth [1] with time and $N$. Thus the use of pruning and merging is very important.

### B. Occlusion likelihood integration

Often the probability of detection, $p_{D,t}(x)$ is considered constant or dependent on the signal-to-noise ratio. In the modified version of the PHD filter a probability of target detection based on the occlusion likelihood is used. Thus, the detection likelihood is calculated as the complement of the occlusion likelihood defined in Section III. The new probability of detection is then

$$p_{D,t}^{new}(\mathbf{x}_t) = p_{D,t}(\mathbf{x}_t)\; p(\overline{O^n}) = p_{D,t}(\mathbf{x}_t)\; (1 - p(O^n)) \tag{19}$$

This probability of detection is used in the update step of the PHD filter, i.e. equations (14), (17) and (18).

### C. Sensor and target model for range-only tracking

A single transmitter synchronized with multiple receivers is considered. The time needed for the signal to travel from the transmitter to a target and back to a receiver can be thus accurately measured. Each transmitter-receiver pair is considered to represent a separate sensor. It is also assumed that the location of the transmitter and receivers is known.

The state vector of a target at time $t$ is defined by the Cartesian $(x, y)$ target position coordinates and velocity:

$$\mathbf{x}_t = [x_t, y_t, \dot{x}_t, \dot{y}_t]^T \tag{20}$$

At time instant $t$ we measure the range with respect to each sensor $j$. Thus the observation is defined as $\mathbf{z}_t^{[j]} = r_t$ and the measurement equation at time $t$ is:

$$\mathbf{z}_t^{[j]} = h^{[j]}(\mathbf{x}_t) + w_t^{[j]} \tag{21}$$

where

$$\begin{aligned} h^{[j]}(\mathbf{x}_t) =& \sqrt{(x_t - x^{Tx})^2 + (y_t - y^{Tx})^2} \\ &+ \sqrt{(x_t - x^{Rx_j})^2 + (y_t - y^{Rx_j})^2} \end{aligned} \tag{22}$$

[1]The growth is exponential if $|Z_t^{[1]}| = \ldots = |Z_t^{[N]}|$ and $J_{\gamma,t} = J_\gamma$ is time independent.

and the observation process noise is $w_t^{[j]} \sim \mathcal{N}\left(0, R_t^{[j]}\right)$. The target dynamics is defined as:

$$\mathbf{x}_t = f_{t|t-1}\left(\mathbf{x}_t|\mathbf{x}_{t-1}\right) \tag{23}$$

where $f_{t|t-1}\left(\mathbf{x}_t|\mathbf{x}_{t-1}\right) = \mathcal{N}\left(x; F_{t-1}\mathbf{x}_{t-1}, Q_{t-1}\right)$ is the transition density and the process noise is $v_t \sim \mathcal{N}\left(0; Q_t\right)$. $F_t = \begin{bmatrix} I_2 & dtI_2 \\ O_2 & I_2 \end{bmatrix}$ is the state transition matrix and the covariance is defined as $Q_t = \sigma_v^2 \begin{bmatrix} \frac{dt^4}{4}I_2 & \frac{dt^3}{2}I_2 \\ \frac{dt^3}{2}I_2 & dt^2 I_2 \end{bmatrix}$, where $dt$ is the time interval between two observations, $\sigma_v^2$ is the variance of the process noise, and $I_n$ and $O_n$ denote $n \times n$ identity and zero matrices respectively.

## V. Evaluation and Results

### A. Numerical results

For demonstrating the performance of the described PHD filter with occlusion likelihood incorporation we simulate a scenario with three moving targets. The target trajectories are shown in Fig. 4 where the end state of each trajectory is indicated by a black circle. The sensor transmitter and two receivers are indicated by the black, blue and green triangles, respectively. For simulating the scenario a person is modeled as a circle with radius $0.3\ m$.

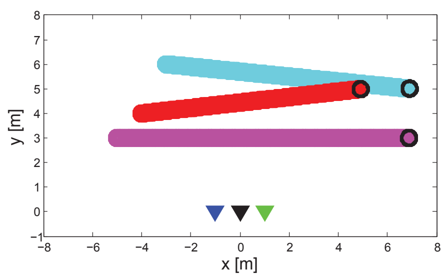


Fig. 4. Simulated tracks for three targets (red, magenta and cyan). Sensor position - transmitter (black), receiver 1 (blue) and receiver 2 (green)

The range observations of the targets including clutter is shown in Fig. 5, where the blue circles represent the observations with respect to the first receiver and the green squares with respect to the second receiver. The red target is shadowed by the magenta target from time 29 to time 50. The cyan target is shadowed by the magenta and red targets from time 44 to time 65. $P(1)$ clutter points uniformly distributed along the range are simulated at each time step, where $P(x) = \frac{e^{-\lambda}\lambda^x}{x!}$ is the Poisson distribution. The measurement noise variance used is $\sigma_w = 0.1\ m$. The probability of target detection by the receivers is assumed constant and same for both receivers, i.e. $p_{D,t}^{[j]}(\mathbf{x}_t) = p_D = 0.95$. Thus the probability of detection in the modified version of the tracker is $p_{D,t}^{new}(\mathbf{x}_t) = p_D\left(1 - p(O^n)\right)$. For the probability of occlusion, a target is modeled as a circle with radius $0.5\ m$. In both versions of the filter a process noise variance $\sigma_v = 10^{-3}$ and probability of survival $p_{S,t}(\mathbf{x}_{t-1}) = p_S = 0.99$ is used.

In the target birth model the intersection points of all range-induced ellipses are used as $x$ and $y$ terms of the mean $m_{\gamma,t}$ of the newborn GMs. The $\dot{x}$ and $\dot{y}$ terms of the mean are 0. The covariance of the newborn targets is $P_{\gamma,t} = diag\left([1, 1, 0.1, 0.1]\right)$. Pruning threshold of $10^{-4}$ and merging threshold 50 is used. The state extraction threshold was set to 0.5.

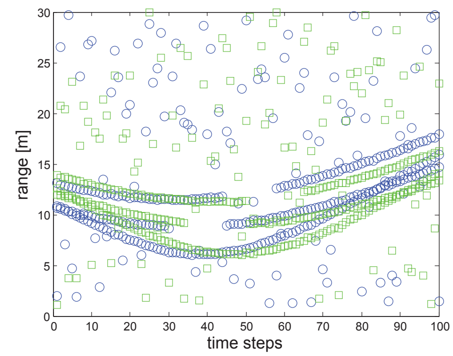


Fig. 5. Targets observations (range as transmitter-target-receiver distance) by $Rx_1$ (blue circles) and $Rx_2$ (green squares)

To evaluate the performance of the PHD filter the OSPA metric as defined in [16] with cut-off $c = 10$ and order $p = 1$ is used. The modified PHD filter (Mod.GMPHD) and the conventional PHD filter (GMPHD) are compared in Fig. 6 where the OSPA metric averaged over 100 Monte Carlo runs for the scenario described above is shown.

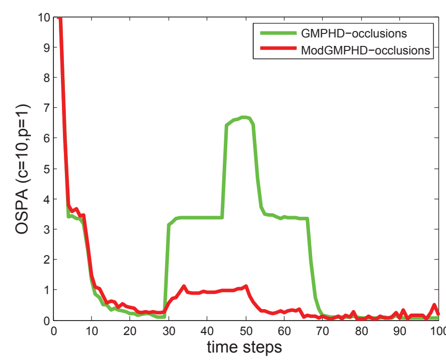


Fig. 6. Average OSPA metric using the PHD filter, GMPHD, (green) and the modified version with occlusion likelihood incorporation, Mod.GMPHD, (red)

As can be observed, using the PHD filter with occlusion likelihood to define the probability of target detection leads to better results, since the filter is able to track the occluded targets (between time step 29 and 65 one or two targets are occluded) and update their state as soon as there is a fitting observation of the previously occluded target. It can be observed that from time step 65 to 69 although all three targets are detected, the GMPHD takes some time until it can correctly estimate the states of all three targets.

## B. Experimental verification

The suggested modification with occlusion likelihood integration is applied to data acquired using one UWB sensor node with transmitter and two receivers placed behind a wall. The UWB sensor node has a bat-type configuration with closely spaced antennas which make the sensor node portable and implementable for hand-held devices. The scenario is as described in Fig. 7. Two persons walk in a room along roughly predefined paths straight to and from the sensor node to the end of the room. The complete ground truth path of the motion of the persons is unfortunately not available and thus a close approximation is used. The UWB module used has $3.5\ GHz$ bandwidth. The measurement rate is $100\ CIR/s$. The UWB module has an M-sequence radar architecture as described in [17]. The feature extraction procedure is range estimation from the received CIRs at each time step as in [9]. The background subtraction method is exponential averaging with forgetting factor $0.85$ which removes the static background reflections. For range detection the constant false alarm rate (CFAR) detector with false alarm probability $0.15$ is applied due to the low signal-to-noise ratio resulting from the signal attenuation when propagating through the wall. To reduce the number of range estimates per target and transmitter-receiver pair to one a hierarchical clustering algorithm is applied. The estimated ranges from the CIR received by receiver 1 are shown in Fig. 8 in blue. The expected range estimates at each time point from a simulation of the same scenario are depicted in black for comparison. As expected, the person closer to the sensor is detected whereas the other person is only sometimes detected. This is accounted to the low signal-to-noise ratio, the attenuation of the UWB signal due to the penetration through wall, and in part to the shadowing imposed by the person closer to the sensor over the rest of the scenario. Based on the approximated ground truth the person closer to the sensor partially occludes the other person throughout the complete measurement time. However, in the first $3\ s$ of the track less than $50\ \%$ of the body is occluded, and thus it can often be detected by the sensor. Starting from the $4^{th}$ second larger portions of the body (more than $50\ \%$) are occluded increasingly. Between the $3^{rd}$ and $4^{th}$ second of the scenario the paths of the two persons are crossing.

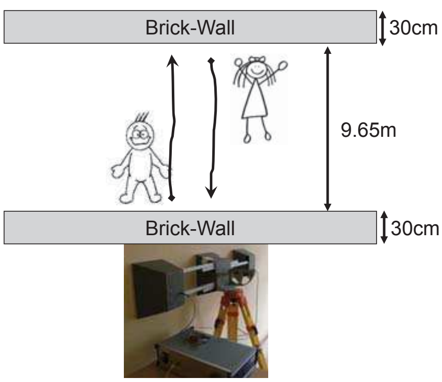


Fig. 7. Scenario schematics

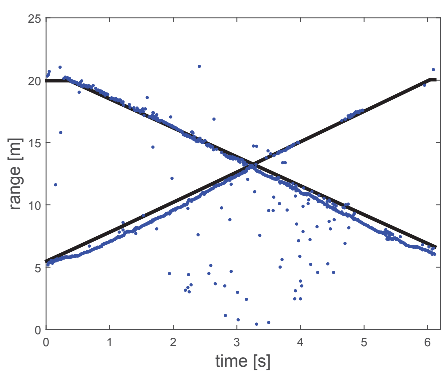


Fig. 8. CFAR range detections (blue) and simulation based expected range estimates (black) for receiver 1 in the two person scenario

Detected targets are modeled as circles with radius $0.7\ m$ and the angular extent parameters are obtained from the model at each time point for each detected target. The radius used to model the target is very large, however it partially accounts for location estimation errors of the detected target. In our scenario location estimation errors arise due to the vicinity of the antennas. The range estimates of both transmitter-receiver pairs are close to each other and the intersection of the range induced ellipses is flat. The accuracy of the occlusion likelihood estimation is highly dependent on the location estimation of the detected targets. Location estimation errors of detected targets can result in predicting high occlusion probability for non-occluded targets or predicting low occlusion probability for occluded targets. Modeling the target with larger radius or based on the error covariance of the current estimate might lead to better results.

For this scenario measurement noise variance $\sigma_w = 0.3\ m$ and process noise variance $\sigma_v = 0.5$ is used. The other filter parameters are same as in the simulation scenario.

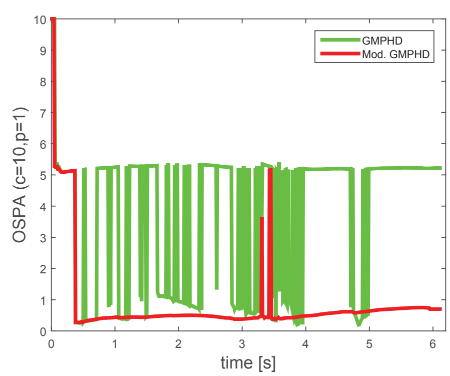


Fig. 9. Average OSPA metric using the PHD filter, GMPHD, (green) and the modified version with occlusion likelihood incorporation, Mod.GMPHD (red)

The OSPA metric with cut-off $c = 10$ and order $p = 1$

of the scenario for the PHD filter and the modified PHD filter is shown in Fig. 9. It should be mentioned that in the implementation of both conventional and modified PHD filter, the number of estimated targets equals the number of surviving mixtures after merging and pruning, and the state estimate of these targets is the mean of those mixtures. Thus, as expected when the paths of the two targets are crossing (around $3.5\ s$), the filter doesn't manage to keep the tracks of both targets. Additionally, the OSPA metric of the conventional PHD filter results in many jumps over the measurement time. As mentioned above one of the targets is always partially occluded by the other. In the first half of the measurement time a smaller portion of the target is occluded and thus it is often detected. However there are still many intervals where the target is not detected (miss detections). Since the PHD filter is not a tracker, if a target state is not updated by an observation for multiple time steps it's weight falls below the estimation threshold and it's state is thus not part of the estimated target states.

Sample of the scenario with the occlusion likelihood at the given time step and the estimated target locations as error ellipses for the conventional and modified PHD filter are shown in Fig. 10. The black circles represent the approximated ground truth location of the persons. The improvement in target location estimation with the modified PHD filter can be clearly observed.

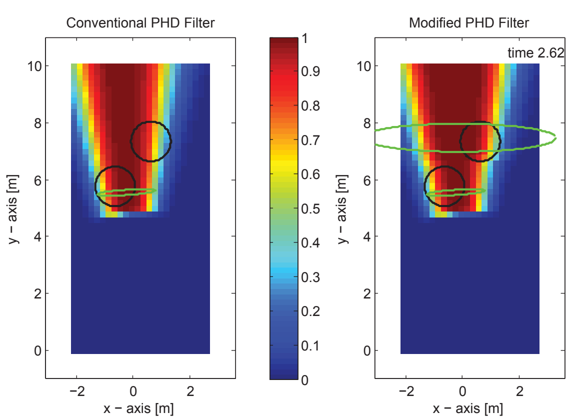


Fig. 10. Sample likelihood without (left) and with (right) occlusion likelihood incorporation with black circles representing the targets positions and green ellipses representing the estimates state covariances of detected targets

## VI. Conclusion

In multiple person localization scenarios, person-induced shadows (or occlusions) lead to target miss-detection. In this paper we describe an occlusion model for defining the occluded area of the scenario at each time point based on the estimated locations of the detected targets. An occlusion likelihood function is described and is later used to calculate the probability of target detection. The modified PHD filter is evaluated on a simulated scenario with three moving persons showing a significant improvement compared to the typical PHD filter where occluded targets are simply discarded after few time steps of non-detection. The modified PHD filter is also applied on experimental data gathered using a bat-type UWB sensor. The improvement in target localization with the modified PHD filter is significant since occluded targets continue to be tracked even tough there are no detections from the sensor. Future improvements by incorporating the occlusion likelihood function in the innovation would limit the error estimate within the occluded region. In addition improvement of the target extent model should result in improved target estimates with lower error covariance.

## References


[1] J. Hoffman, M. Spranger, D. Gohring, and M. Jungel, "Making use of what you don't see: negative information in Markov localization," in *Intelligent Robots and Systems, 2005. (IROS 2005). 2005 IEEE/RSJ International Conference on*, Aug 2005, pp. 2947–2952.

[2] S. Thrun, W. Burgard, and D. Fox, *Probabilistic robotics*. MIT press, 2005.

[3] K. Tischler and H. Vogt, "A sensor data fusion approach for the integration of negative information," in *Information Fusion, 2007 10th International Conference on*, July 2007, pp. 1–7.

[4] W. Koch, "On exploiting 'negative' sensor evidence for target tracking and sensor data fusion," *Information Fusion*, vol. 8, no. 1, pp. 28–39, 2007.

[5] M. Powers, R. Ravichandran, F. Dellaert, and T. Balch, "Improving multirobot multitarget tracking by communicating negative information," in *Multi-Robot Systems. From Swarms to Intelligent Automata Volume III*, L. Parker, F. Schneider, and A. Schultz, Eds. Springer Netherlands, 2005, pp. 107–117. [Online]. Available: http://dx.doi.org/10.1007/1-4020-3389-3_9

[6] A. Andriyenko, S. Roth, and K. Schindler, "An analytical formulation of global occlusion reasoning for multi-target tracking," in *ICCV Workshops*. IEEE, Nov. 2011, pp. 1839–1846.

[7] K. Wyffels and M. Campbell, "Negative observations for multiple hypothesis tracking of dynamic extended objects," in *American Control Conference (ACC), 2014*, June 2014, pp. 642–647.

[8] S. Jovanoska and R. Thoma, "Multiple target tracking by a distributed UWB sensor network based on the PHD filter," in *Information Fusion (FUSION), 2012 15th International Conference on*, 2012, pp. 1095–1102.

[9] S. Jovanoska, R. Zetik, R. Thoma, F. Govaers, K. Wilds, and W. Koch, "Device-free indoor localization using a distributed network of autonomous UWB sensor nodes," in *Sensor Data Fusion: Trends, Solutions, Applications (SDF), 2013 Workshop on*, Oct 2013, pp. 1–6.

[10] D. Urdzik, R. Zetik, D. Kocur, and J. Rovnakova, "Shadowing effect investigation for the purposes of person detection and tracking by UWB radars," in *Microwave Conference (GeMiC), 2012 The 7th German*, 2012, pp. 1–4.

[11] S. Jovanoska, F. Govaers, R. Thoma, and W. Koch, "Dynamic occlusion handling in the phd filter for range-only tracking: Proof of concept," in *Sensor Data Fusion: Trends, Solutions, Applications (SDF), 2014*, Oct 2014, pp. 1–6.

[12] R. Mahler, "Multitarget Bayes filtering via first-order multitarget moments," *IEEE Trans. Aerosp. Electron. Syst.*, vol. 39, no. 4, pp. 1152–1178, Oct. 2003.

[13] ——, *Advances in Statistical Multisource-multitarget Information Fusion*. Artech House, 2014, ch. Multisensor PHD and CPHD Filters.

[14] N. T. Pham, W. Huang, and S. Ong, "Multiple sensor multiple object tracking with GMPHD filter," in *Information Fusion, 2007 10th International Conference on*, July 2007, pp. 1–7.

[15] B.-N. V. Vo and W.-K. Ma, "The Gaussian mixture probability hypothesis density filter," *IEEE Trans. Signal Process.*, vol. 54, no. 11, pp. 4091–4104, Nov. 2006.

[16] D. Schuhmacher, B.-T. Vo, and B.-N. Vo, "A consistent metric for performance evaluation of multi-object filters," *Signal Processing, IEEE Transactions on*, vol. 56, no. 8, pp. 3447–3457, Aug 2008.

[17] R. Zetik, M. Kmec, J. Sachs, and R. S. Thomä, "Real-time mimo channel sounder for emulation of distributed ultrawideband systems," *International Journal of Antennas and Propagation*, 2014.